



Modelling End-of-Season Soil Salinity in Irrigated Agriculture Through Multi-temporal Optical Remote Sensing, Environmental Parameters, and In Situ Information

Murodjon Sultanov¹ · Mirzakhayot Ibrakhimov¹ · Akmal Akramkhanov² · Christian Bauer³ · Christopher Conrad^{3,4}

Received: 20 October 2018 / Accepted: 11 January 2019 / Published online: 7 February 2019
© Deutsche Gesellschaft für Photogrammetrie, Fernerkundung und Geoinformation (DGPF) e.V. 2019

Abstract

Accurate information of soil salinity levels enables for remediation actions in long-term operating irrigation systems with malfunctioning drainage and shallow groundwater (GW), as they are widespread throughout the Aral Sea Basin (ASB). Multi-temporal Landsat 5 data combined with GW levels and potentials, elevation and relative topographic position, and soil (clay content) parameters, were used for modelling bulk electromagnetic induction (EMI) at the end of the irrigation season. Random forest (RF) regression was applied to predict *in situ* observations of 2008–2011 which originated from a cotton research station in Uzbekistan. Validation, i.e. median statistics from 100 RF runs with a holdout of each 20% of the samples, revealed that mono-temporal (R^2 : 0.1–0.18, RMSE: 16.7–24.9 mSm^{-1}) underperformed multi-temporal RS data (R^2 : 0.29–0.45; RMSE: 15.1–20.9 mSm^{-1}). Combinations of multi-temporal RS data with environmental parameters achieved highest accuracies (R^2 : 0.36–0.50, RMSE: 13.2–19.9 mSm^{-1}). Beside RS data recorded at the initial peaks of the major irrigation phases, terrain and GW parameters turned out to be important variables for the model. RF preferred neither raw data nor spectral indices known to be suitable for detecting soil salinity. Unexplained variance components result from missing environmental variables, but also from processes not considered in the data. A calibration of the EMI for electrical conductivity and the standard soil salinity classification returned an overall accuracy of 76–83% for the period 2008–2011. The presented indirect approach together with the *in situ* calibration of the EMI data can support an accurate mapping of soil salinity at the end of the season, at least in the type of irrigation systems found in the ASB.

Keywords Soil salinity · Electromagnetic induction · Irrigated agriculture · Multi-temporal · Environmental parameters · Landsat

Zusammenfassung

Modellierung der Bodensalinität am Ende einer Bewässerungssaison durch multi-temporale optische Fernerkundungsdaten, Umweltvariablen und in situ Informationen. Genaue Informationen über den Salzgehalt des Bodens ermöglichen Sanierungsmaßnahmen in etablierten Bewässerungssystemen mit mangelhafter Entwässerung und flachem Grundwasser (GW), wie sie etwa im gesamten Aralseebecken (ASB) verbreitet sind. Landsat-5-Daten aus mehreren Zeiträumen wurden mit GW-Werten und -Potentialen, Höhe und relativer topographischer Position sowie Bodeninformation (Ton Gehalt) kombiniert, um die elektromagnetische Induktion (EMI) am Ende der Bewässerungssaison zu modellieren. Random Forest (RF) Regression wurde angewendet, um *in situ* Beobachtungen von 2008–2011 vorherzusagen, die von einer Baumwollforschungsstation in Usbekistan stammen. Die Medianstatistik der Validierung von 100 RF-Läufen mit einem Holdout von jeweils 20% der Proben zeigte, dass mono-temporale (R^2 : 0,1–0,18; RMSE: 16,7 mSm^{-1} –24,9 mSm^{-1}) multi-temporalen Fernerkundungsdaten unterlegen waren (R^2 : 0,29–0,45; RMSE: 15,1 mSm^{-1} –20,9 mSm^{-1}). Optimale Ergebnisse wurden aber durch Kombinationen von multi-temporalen Fernerkundungsdaten und Umweltvariablen erzielt (R^2 : 0,36–0,50, RMSE: 13,2 mSm^{-1} –19,9 mSm^{-1}). Neben den Fernerkundungsdaten, die zu Beginn der Hauptbewässerungsphasen aufgezeichnet wurden, erwiesen sich die Gelände- und GW-Parameter als wichtige Variablen für das Modell. RF bevorzugte weder Rohdaten noch

Spektralindizes, die vorwiegend zum Nachweis der Salzgehalte im Boden geeignet sind. Unerklärte Varianzanteile resultieren aus fehlenden Umweltvariablen, aber auch aus in den Daten nicht berücksichtigten Prozessen. Eine Kalibrierung der EMI auf die elektrische Leitfähigkeit und die Klassifizierung nach Standard-Bodensalzgehalt ergab eine Gesamtgenauigkeit von 76% bis 83% für den Zeitraum 2008 – 2011. Der vorgestellte indirekte Ansatz zusammen mit der *in situ* Kalibrierung der EMI-Daten kann eine genaue Kartierung des Bodensalzgehaltes am Ende der Saison unterstützen, zumindest in der Art von Bewässerungssystemen, wie sie im ASB vorkommen.

1 Introduction

Soil salinity in irrigated crop production systems is highly dynamic in space and time. Irrigation and leaching events cause lateral inflow, but also downward movements and lateral outflow of salt through the drainage system. In turn, capillary rise returns the salt from the filtration/ground water up to the soil layer (Hillel 2000). Reduced vegetation growth and crop failure are the consequence. In irrigation systems without functioning drainage and with shallow groundwater (GW) levels and that operate over a certain time span, this usually leads to permanent salinization of the soil layer (Abrol et al. 1988). This constellation of poor drainage of salts occurs worldwide and threatens in particular the irrigated crop production systems of the Aral Sea Basin (ASB, Qadir et al. 2009).

Numerical modelling of the prescribed water and salt movements may be an option to quantify soil salinization accurately. At the same time, this method is data and computation intensive as well as challenging for assessments over extensive areas (Bastiaanssen et al. 2007). Another option to quantify soil salinity is the use of remote sensing (RS) techniques. For instance, spectra of salt minerals exhibit distinctive absorption features and hyperspectral methods suit for predicting the concentration of many salt types in soil samples under laboratory conditions (Farifteh et al. 2008). Also mapping of different salinity levels in the top soil layer becomes possible when using field spectra or hyperspectral RS data and statistical methods (Farifteh et al. 2007). However, the authors state that dynamic factors such as vegetation cover or soil moisture certainly influences the explanatory power of such so-called direct assessments of soil salinity through RS. These dynamics are particularly high in agricultural areas.

Alternatively, in many salinity affected irrigated regions reduced crop growth indirectly indicates salinity in soils (e.g. Metternicht and Zinck 2003; Abbas and Khan 2007; Farifteh et al. 2007; Lobell et al. 2007), crop growth status has been investigated to map soil salinity through mainly multispectral RS data with statistical models (Allbed and Kumar 2013).

A variety of spectral indices that can measure greenness and density of vegetation with or without compensation for differences in soil properties or that target directly on salinity were tested (e.g. Abbas and Khan 2007; Eldeiry and Garcia 2008; Azabdaftari and Sunar 2016). Interestingly, the usage of water-related indices that include the shortwave infrared

information such as the normalized difference infrared index (NDII) is rare, even though water stress and wilting are consequences of increased soil salinity (Brower et al. 1985).

Numerous univariate and multivariate regression models were applied for indirect quantification of soil salinity with RS data, but in many cases with moderate success only (Allbed and Kumar 2013). For instance, Azabdaftari and Sunar (2016) report high coefficient of determination ($R^2 = 0.78$) when using the salinity index, but admit that without removing some samples from the data set R^2 dropped to 0.37. Reasoning for the selection was not given and the analysis was done without separation of extra data for validation. It may be worthwhile to investigate the effect of non-linear methods such as partial least square regression or artificial neural networks which achieved striking explanatory power in direct soil salinity assessments (Farifteh et al. 2007). In addition, not all crops have the same salt tolerance, and reduced vegetation growth in irrigation systems can also be driven by water scarcity and drought, low nutrient content of the soils, and other yield reducing factors (Ittersum et al. 2013). To disentangle potential factors of limited crop growth challenges indirect assessments of soil salinity with remote sensing (Allbed and Kumar 2013).

The use of environmental parameters that are well-known drivers of soil salinization, also in combination with RS data, is another possibility for analysing saline soils (Akramkhanov et al. 2011; Akramkhanov and Vlek 2012; Asfaw et al. 2018) or for predicting the risk of soil salinization (Huang et al. 2016). GW table for instance is used as indication for critical levels for capillary rise. Topography can point at locations, which are close to the GW table and hence more likely effected by capillary rise than other areas. In such studies, RS data served as summary indicator (e.g. Akramkhanov and Vlek 2012) but to a limited extend only, e.g. a reduced number of bands.

Another potential shortcoming of previous indirect salinity assessments (Metternicht and Zinck 2003), irrespectively if with or without environmental parameters or if with multispectral (e.g. Azabdaftari and Sunar 2016) or hyperspectral data (e.g. Dehaan and Taylor 2002), is the consideration of single dates and single seasons (Lobell et al. 2007). Even though Lobell et al. (2007) could not establish a statistical link of multi-annually modelled crop yield to soil salinity (due to other yield reducing factors), this study applies a multi-temporal approach. The goal of this study is to utilize

multi-temporal RS data (raw bands and spectral indices) and non-linear random forest for assessing soil salinity levels at the end of cropping season. At that time, vertical processes are reduced after the irrigation events cease and the salinity build-up in the soils become more discernible (Akramkhanov et al. 2014). It is hypothesized that environmental parameters, which indicate soil salinity such as soil texture (clay content), terrain (elevation and topographic position), and GW information (levels and potentials), can optimize such assessments through their ability to discriminate soil salinity from other drivers of reduced crop growth conditions. Experiments were conducted in the Khorezm region of Uzbekistan, a well-known salinity-exposed province in the ASB (Ibrakhimov et al. 2007).

2 Materials and Methods

2.1 Study Area

The Khorezm province is located between 41°N–42°N and 60°E–61°E, ~200 km from the Aral Sea (Fig. 1). The climate of the region is continental, characterized by annual average potential evapotranspiration of 1400 mm that exceeds precipitation of 92 mm by far (Conrad et al. 2012). Agriculture heavily relies on irrigation water coming from the Amu Darya River. Upland cotton (*Gossypium hirsutum*) and winter wheat (*Triticum aestivum*) are the area-dominant crops (Conrad et al. 2016a). Cotton is usually grown from April through September/October. The peak irrigation period is June–August. Irrigation of winter wheat starts in November and ends in May. Leaching period is in winter.

The majority of cropped areas are irrigated through furrows and basins. Water is supplied through a mainly unlined irrigation network. The irrigation of these water-intensive crops and seepage from the canal networks are the primary causes of the groundwater (GW) rise and subsequent soil moisture contribution (Jabbarov 1990). Silty loam, loam, and sandy loam dominate the soil texture in the region occupying 55%, 13%, 12%, respectively, according to the USDA classification (Akramkhanov et al. 2012).

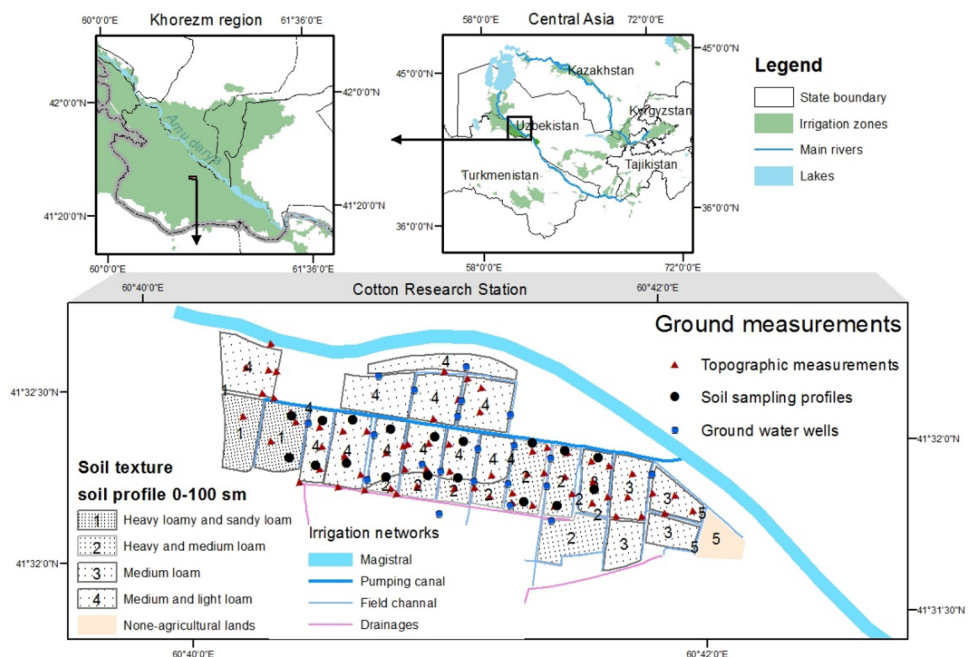
Detailed fieldworks were conducted at the Cotton Research Station (CRS) of the Pakhtakor Water Consumers Association (Fig. 1). The total irrigated area of CRS amounts to 145 ha. According to Akramkhanov et al. (2014), the salinity levels in CRS are mainly low to moderate indicated by electrical conductivity (EC) levels in the range of 0.6–10.9 dSm⁻¹.

2.2 Remote Sensing Data and Calculation of Indices

Landsat 5 TM surface reflectance data (Path 160/Row 31) were obtained from the USGS archive (<http://earthexplorer.usgs.gov>). The selected Level-2 data are atmospherically corrected through the Landsat Ecosystem Disturbance Adaptive Processing System (LEDAPS, Masek et al. 2013). Cloud-free observations of the vegetation seasons (April–November) 2008–2011 included 23 data sets. After some tests, in total 14 data sets with a clear vegetation signal (end of May–October) were selected for modelling (Table 1). Data from the initial vegetation period, where soils dominate the RS signal, were omitted.

Because crops experience stress under saline soil conditions (Allbed and Kumar 2013), normalized difference

Fig. 1 Upper part: location of the Khorezm province in the Aral Sea Basin (Central Asia), lower part: the Cotton Research Station, soil texture information and location of ground measurements



vegetation index (NDVI) and soil-adjusted vegetation index (SAVI) showing the density and greenness of vegetation were calculated and added to the six raw bands of Landsat 5, which range from the visible to the short-wave infrared spectrum. Two indicators for water stress, i.e. normalized difference infrared index (NDII) and NDII2, supplemented the data sets. The names of these indices vary in literature, e.g. the NDII is also known as Land Surface Water Index (LSWI, e.g. Xiao et al. 2005). The NDII2 refers to LSWI₂₁₀₅ (Xiao et al. 2005) or NDII7 when applied to MODIS band 7 (AghaKouchak and Farahmand 2015) and is better known as normalized burn ratio (Keeley 2009). However, all indices depend on the sensor specification, i.e. the wavelength range and sensitivity for the selected band. Table 2 contains equations and references for the selected indices.

2.3 Soil Salinity Measurements

Electromagnetic induction meters are widely used for in situ salinity measurements in irrigation systems, as it is more efficient to cover large areas than single samples together with laboratory analysis of EC (Hendrickx et al. 1992). However, EMI can only be seen as a proxy of soil salinity (e.g. Huang et al. 2016). Akramkhanov and Vlek (2012) give examples for the statistical relation of EMI and EC under different soil texture conditions. For the study area, a

Table 1 Acquisition dates of Landsat 5 images and corresponding electromagnetic induction (EMI) surveys during the vegetation period of 2008–2011 in the Cotton Research Station (CRS) area

	2008	2009	2010	2011
Landsat 5	4 July	6 July	9 July	25 May
	20 July	22 July	10 August	12 July
	22 September	8 September	11 September	
	8 October	10 October	27 September	
EMI measurement period	2–3 October	15 October	25 October	15 October

Table 2 Remote sensing indices used for estimation of soil salinity, red, nir, swir1, and swir2 refers to wavelength ranges of Landsat 5 TM bands 3 (0.63–0.69 μm), 4 (0.76–0.90 μm), 5 (1.55–1.75 μm), and 7 (2.08–2.35 μm), respectively

Spectral Index	Equation	Reference
Normalized Difference Vegetation Index (NDVI)	$\text{NDVI} = \frac{\text{nir} - \text{red}}{\text{nir} + \text{red}}$	Rouse et al. (1974)
Soil Adjusted Vegetation Index (SAVI)	$\text{SAVI} = \frac{1.5 \times (\text{nir} - \text{red})}{\text{nir} + \text{red} + 0.5}$	Huete (1988)
Normalized Difference Infrared Index (NDII)	$\text{NDII} = \frac{(\text{nir} - \text{swir1})}{(\text{nir} + \text{swir1})}$	Xiao et al. (2005)
Normalized Difference Infrared Index 2 (NDVII2)	$\text{NDII2} = \frac{(\text{nir} - \text{swir2})}{(\text{nir} + \text{swir2})}$	

combined set of 142 sample pairs of EMI and EC taken at different time periods was thought to provide relationship that is close to real-world situation, even though coefficient of determination (R^2) of 0.44 between log-transformed EMI measurements and EC was rather low (Akramkhanov et al. 2014).

Field data collection occurred in 2008–2011, in the end of the season each. Soil salinity was sampled using the EM-38 (Geonics Limited, Canada). The measurements originate from ten fields with average size of ca. 7 ha each. The EMI measurements were conducted in vertical dipole mode, sensing depth up to 1.5 m with the highest sensitivity depth at 0.4 m. The EMI device was coupled with GPS (average accuracy 3–5 m). Figure 2 shows the measurement transects 2008–2011 and the crop distribution. Most of the fields were cultivated with cotton and some with maize. Wheat occurred in rotation with other summer crops (mainly maize). Details of the sampling campaigns and the resulting data are available in Akramkhanov et al. (2014). The mean EMI in survey data, aggregated within 30 m pixels of Landsat, ranged from 44–53 mSm^{-1} to 51–74 mSm^{-1} .

2.4 Environmental Parameters

2.4.1 Elevation and Topographic Position

Elevation measurements were taken at 65 locations evenly distributed in the CRS (Fig. 1). Elevation in the CRS ranged between 99.5 to 100.5 m above sea level (mean 99.88 $\text{m} \pm 0.27$ m). The elevation map (Fig. 3) was obtained by interpolation between data points using inverse distance weighted (IDW) technique (Shepard 1968). Local topography of farmland surface declines slightly from east to west and to southern west.

To consider the variations in the generally flat terrain, the topographic position index (TPI) was applied (Fig. 3). It measures the relative topographic position, i.e. it returns terrain properties in relation to the neighbourhood and indicates if a certain point is located in depression, on slopes, on hills, or in flat area. TPI is the difference between elevation at the central point (z_0) and at points (z_i) within a predetermined radius (R) around the central point (Majka et al. 2007)

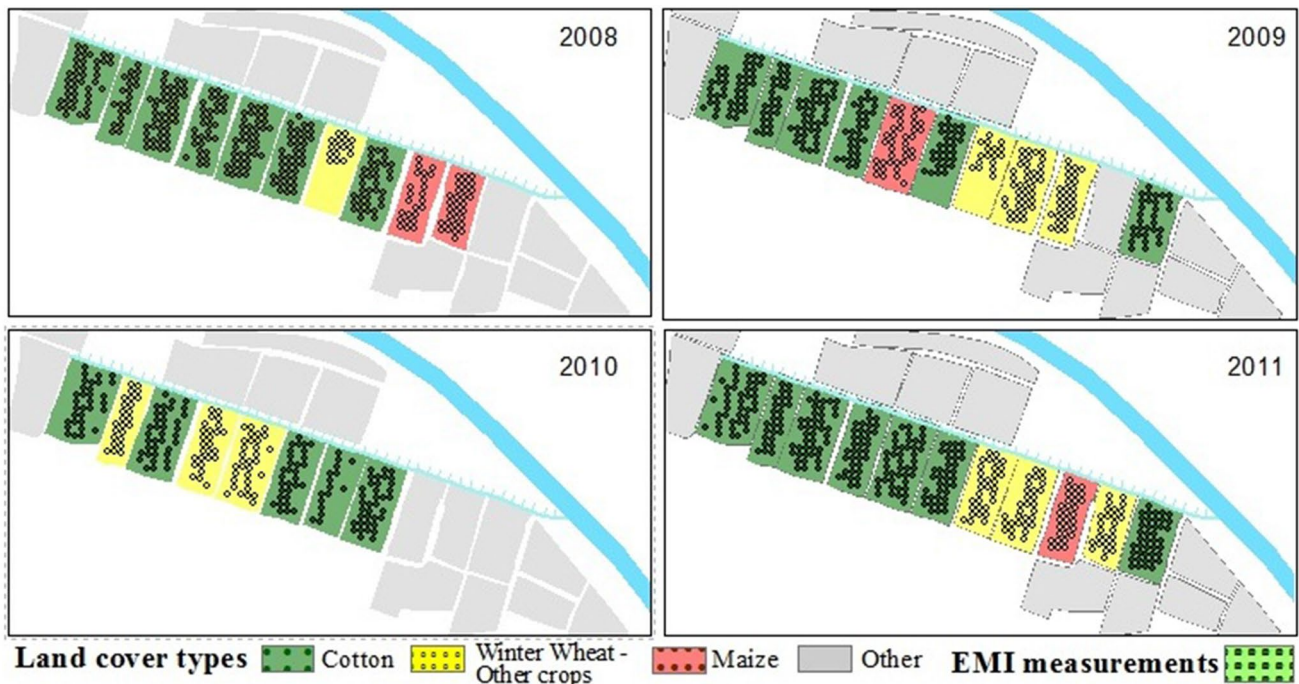


Fig. 2 Location of electromagnetic induction (EMI) samples in the Cotton Research Station, Khorezm, 2008–2011

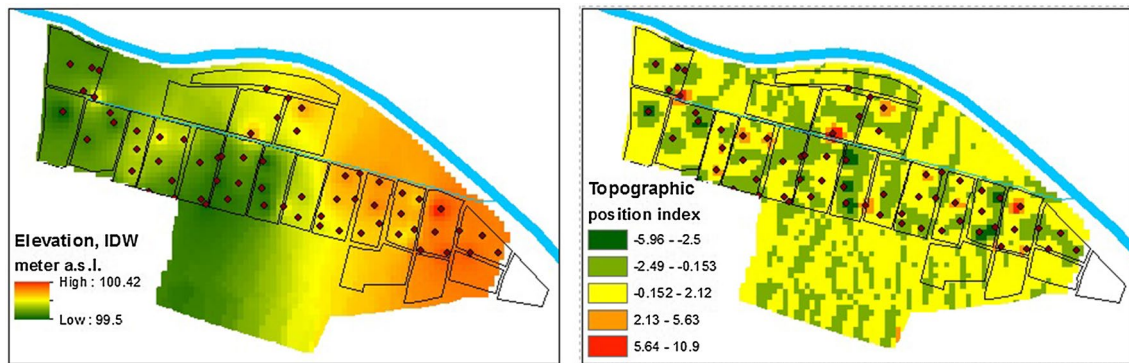


Fig. 3 Elevation (left part) and topographical position index (TPI, right part) of the study region

and was computed based on the IDW output according to Eq. (1).

$$TPI = z_0 - \frac{\sum_{i=1}^n z_i}{n} \tag{1}$$

2.4.2 Groundwater Levels and Potential

In Khorezm, intensive irrigation events cause rapidly rising groundwater (GW) tables that accelerate accumulation of salts in soil root zone. Ibrakhimov et al. (2007) referred to Russian sources and stated that salinization takes place when GW with salinity over 3 g l⁻¹ rises above 2.0 m below

the ground surface and assumed 1.5 m as benchmark for less saline GW. Data on GW table were obtained from 21 monitoring wells with automatic recording devices. However, because official GW monitoring in Uzbekistan is conducted at the peak of the vegetation period, only groundwater levels of early August were included. The GW table data from monitoring wells (GWT) were interpolated using IDW method and subtracted from the topographic map to obtain the spatial distribution of the GW potential energy (GWP). Figure 4 shows the spatial distribution of GWT and GWP and their variations in 2008–2011. Despite measured during the peak of irrigation, GWT in the CRS only seldom and in

some places reached critical levels described by Ibrakhimov et al. (2007).

2.4.3 Soil Texture (Clay Content)

Soil texture, especially the clay content, influences soil salinity (Huang et al. 2016). Thus, physical clay content was selected as indicator for soil salinity in this study and local maps of soil texture provided by the GIS-laboratory at the NGO KRASS in Urgench, Khorezm were translated into that parameter. The spatial distribution of the soil texture is shown in Fig. 1, whilst tabular information is summarized in Table 3. The texture classes in the region include “heavy

loam” (clay content > 60%), “heavy and medium loam” (45–60%), “heavy and sandy loam” (35–45%), “medium loam” (30–45%), and “light loam” (< 30%). The physical clay content refers to the former Soviet classification system, which classifies particle size below 0.001 mm as clay (Stolbovoi 2000). Only the information from 30 to 100 cm was utilized (Table 3). The data were entered as ordinal variable (classes 1–4) into the model indicating the different levels of clay content in descending order.

Fig. 4 Groundwater tables (GWT, left part), and ground-water potential (GWP, right part) at the cotton research station in Khorezm, Uzbekistan, as measured and interpolated in August; *asl.* above sea level

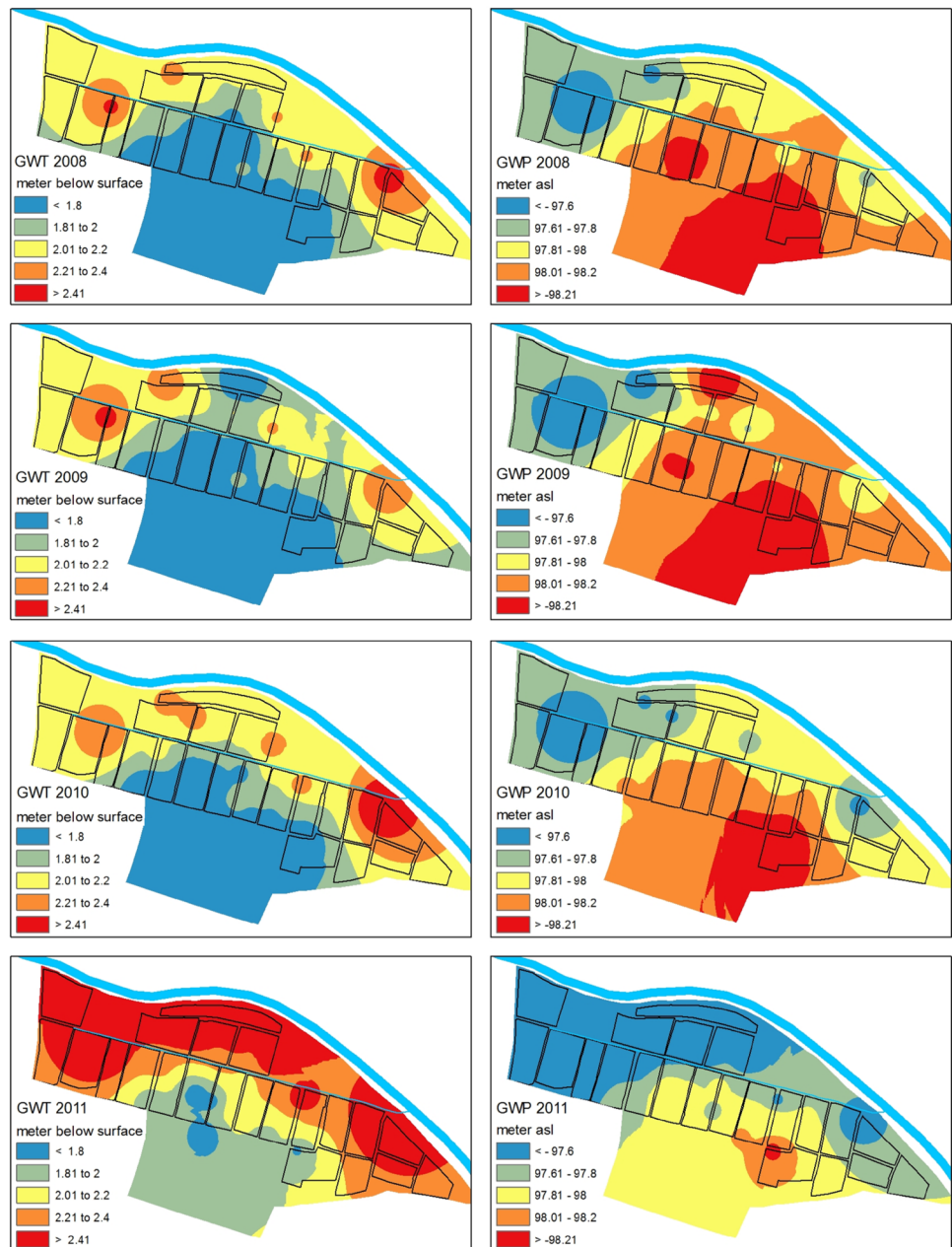


Table 3 Typical combinations of soil texture at different layer depths occurring in the study region

Class	Soil texture		
	0–30 cm	30–100 cm	100–200 cm
1	Heavy loam	Heavy and medium loam	Medium loam
2	Heavy loam	Heavy loam and sandy loam	Sandy loam
3	Medium loam	Medium loam	Medium loam
4	Medium loam	Medium and light loam	Light and sandy loam
5	Unused land		

2.5 Random Forest Regression

For modelling soil salinity, random forests (RF) regression as introduced by Breiman (2001) was applied using the randomForest package in R (<http://R-project.org>). An RF is an ensemble of classification and regression trees (CART). Each CART is built from a sample drawn with replacement (bootstrap) from the training set. CART splits each node using the best among a subset of predictors randomly chosen at that node, i.e. the optimally separating pair of predictor and threshold. As splitting criterion, a threshold value S is chosen such that the term in Eq. (2) is minimized.

$$\sum_{y_i|x_i \leq S} (y_i - \bar{y})^2 + \sum_{y_i|x_i > S} (y_i - \bar{y})^2, \quad (2)$$

where y refers to the dependent variable and x to the predictor. \bar{y} denotes the mean of all elements y_i and the threshold value S can take any value of the predictor variable x .

As a result of the randomness of predictor and sample selection, the bias of the ensemble usually slightly increases but, due to averaging, its variance decreases, usually more than compensating for the increase in bias, hence yielding an overall better model (Breiman 2001). The decision to set the number of CARTs in RF to 500 followed a recommendation by Gislason et al. (2006).

The input covariates as explanatory variables included raw bands (1–6) of Landsat 5 images (Table 1) as well as the vegetation and water indices described in Table 2. Additional RF runs were conducted using four environmental covariates: topography referred to as TPI, groundwater table (GWI), and groundwater potential (GWP), and physical clay content (soil texture). Altogether, four sets of models with different combination of input data were constructed based on (a) single image (si), where the maximum NDVI period was selected as input (~July), (b) multiple images (mi) within developing and mid-stages of crop development (four scenes each year), and single images in combination with environmental parameters (env), e.g. (c) si + env, and (d) mi + env.

2.6 Variable Importance

For each RF, the importance of each variable was assessed through the so-called “%IncMSE” procedure (Breiman 2001). This procedure tests the importance of each variable by randomly permuting the variable values before running the model. If a variable is important, this permutation negatively influences prediction and the model results hence in a higher mean square error (MSE).

2.7 Validation

Repeated sub-sampling technique served for validation, i.e., for each model with and without environmental indicators, 100 iterations were applied. Every run excluded a random subset of 20% of samples (holdout) to assess the accuracy and the stability of the model. To estimate the accuracy of each model, both the coefficient of determination (R^2 , Eq. 3) and the root mean square error (RMSE, Eq. 4) were applied to compare observed and modelled soil salinity of these random subsets:

$$R^2 = 1 - \frac{\sum_{i=1}^n (y_i - \hat{y}_i)^2}{\sum_{i=1}^n (y_i - \bar{y})^2}, \quad (3)$$

$$\text{RMSE} = \sqrt{\frac{\sum_{i=1}^n (y_i - \hat{y}_i)^2}{n}}, \quad (4)$$

where \bar{y} is the mean of the observed data, and y_i and \hat{y}_i refer to the modelled and observed parameters, respectively. R^2 is a measure of the explained variation, indicating how close the predicted values deviate from the measurements. The RMSE is the square root of the variance of the residuals, pointing to the overall fit of the regression model.

3 Results

3.1 Validation

The random forest (RF)-based regression analysis received (for the 20% of independent data) coefficients of determination (R^2) between >0–0.75. The boxplots (Fig. 5) show below (above) the black bold line the 25–50% (50–75%) percentile of R^2 which returned from the 100 RF runs. Median R^2 (bold line) of single data sets without environmental information (si) was lower than that of multiple data sets (mi). The use of environmental parameters increased the accuracy of the model in all cases (si + env, mi + env), in particular in 2011, where only few data sets were available

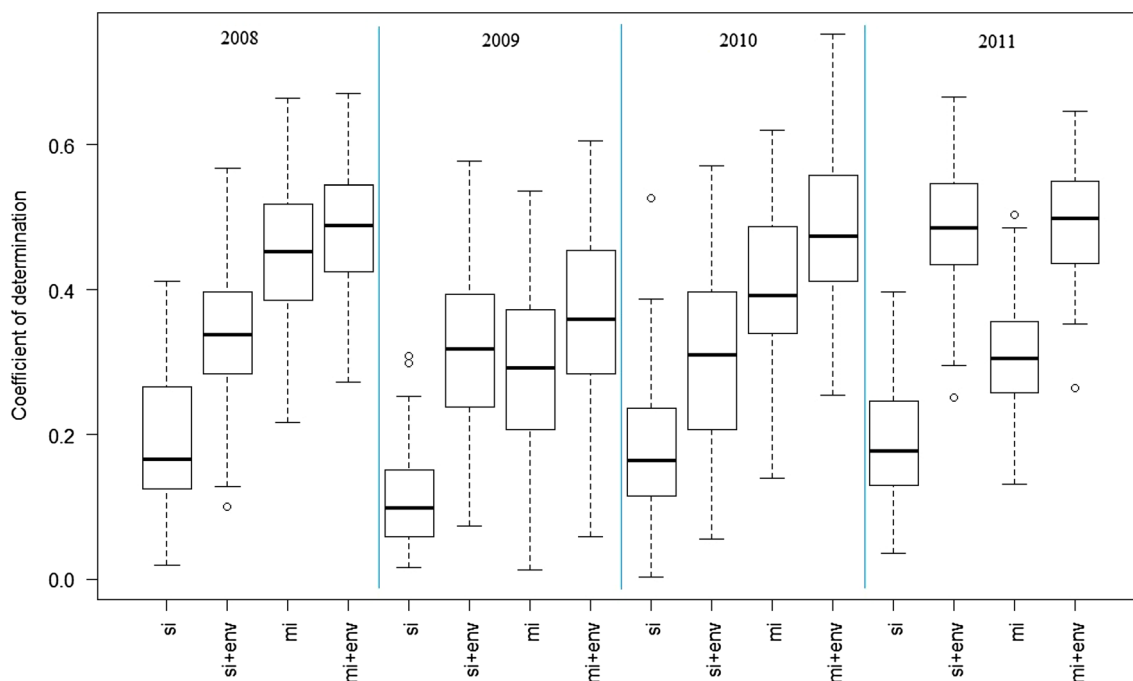


Fig. 5 Coefficients of determination (R^2) of the regression analysis of soil salinity against mono- and multi-temporal remote sensing indices with and without environmental parameters using random forest

(RF); *si* single image, *mi* multiple images, *env* environmental parameters; the boxplots indicate the variability of the 100 RF runs applied to each set of variables

during the irrigation phase in July and August. In 2009, lowest accuracy levels were recorded.

RMSE median ranged from 14 to 25 mSm^{-1} (Fig. 6). Summary statistics of RMSE extracted from 100 RFs show similar tendency to R^2 but also slight variations. Despite a reduced model fit (R^2) in 2011, low median RMSE ($< 18 \text{ mSm}^{-1}$) indicate more accurate predictions in contrast to 2010, when the RMSE median exceeded 20 mSm^{-1} . Modifications of RF settings (number of trees grown, or changes in the number of random feature selection) altered the results only negligibly.

3.2 Driving Factors (Variable Importance Analysis)

Variable importance of the individual factors in the overall relationship of RS data and environmental parameters (*mi + env*) with soil salinity (EMI) was averaged over the 100 RFs (Fig. 7). Environmental parameters (GWP, GWT, and TPI) contributed remarkably, whereas soil texture, i.e. physical clay content, could not increase model performance in most cases. In 2009 and 2011, groundwater information (GWT and GWP) played a major role and all other factors showed reduced importance. The spectral information (RS data) does not show a clear pattern in its variable importance. Only spectral bands or indices of early–mid July appeared among the most important predictors, in particular in 2008 and 2010.

3.3 Spatial Distribution of Soil Salinity (EMI)

Maps of soil salinity expressed by EMI data were produced for the four observation years by utilizing the annual RF models (Fig. 8). In 2010, the lowest soil salinity was predicted throughout the CRS. Comparatively high values were observed in 2009 and 2011. Visual observation confirms that the soil salinity patterns in the CRS resemble each year however with some variation. Hotspots of salinity occur in the most western and eastern parts of the study area (fields 28 and 27). Dynamic developments occurred on fields 12 and 13, and field 20 exhibits increasing trends of EMI 2008–2011.

4 Discussion

4.1 Validation

The validation based on repeated sub-sampling indicates moderate prediction performance of the random forest (RF) model approach based on RS data. Other authors reported higher performance of the indirect prediction method via RS vegetation parameters. For instance, Asfaw et al. (2018) and Azabdaftari and Sunar (2016) observed $\sim 0.8 R^2$ between spectral information (raw bands, indices, no environmental parameters) and soil salinity. However, their assessments

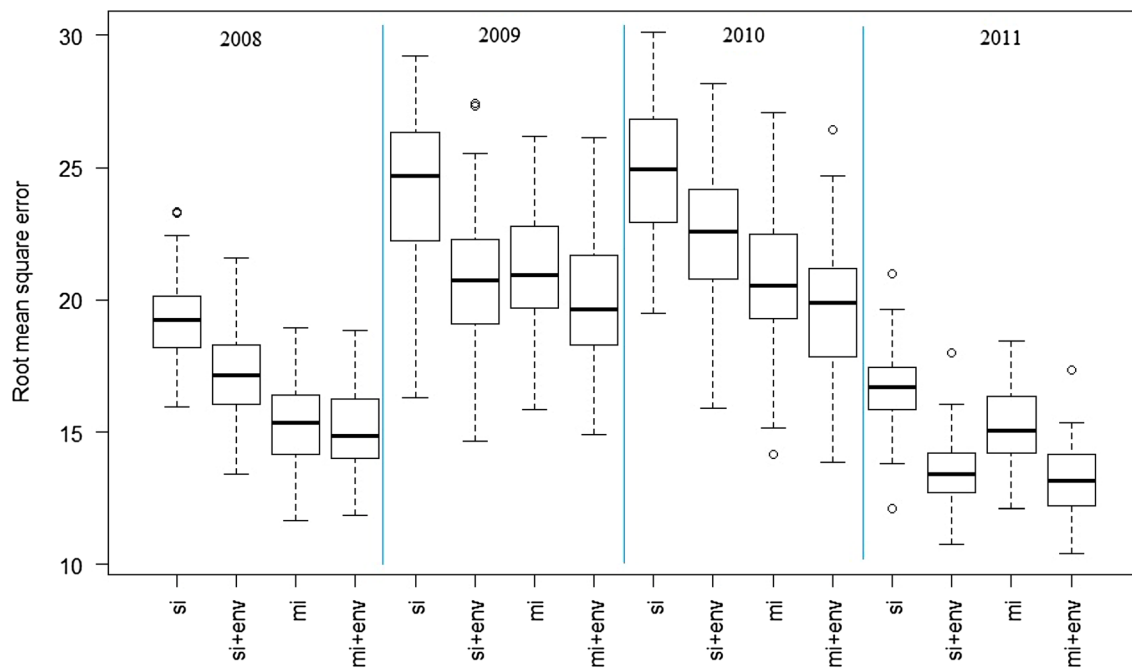


Fig. 6 Root mean square error (RMSE) of the regression analysis of soil salinity against mono- and multi-temporal remote sensing indices with and without environmental parameters using random forest

(RF); *si* single image, *mi* multiple images, *env* environmental parameters; the boxplots indicate the variability of the 100 RF runs applied to each set of variables

were based on training samples only rather than on independent data. For instance, in this study, accuracy assessments based on training samples only exceeded an R^2 of 0.95 (not shown in detail). Such assessments are less meaningful as they measure the relation of the parameters with soil salinity at the selected points but do not assess the validity of the model for prediction. For instance, Akramkhanov et al. (2011) analysed the relationship between numerous environmental parameters and soil salinity (bulk salinity measured through the EM-38 device) and found an R^2 of 0.48 based on the entire data set (not independent reference data). They included—in comparison to the study at hand—a large set of terrain and soil parameters for prediction, among others soil texture as well as one RS data set (Landsat 7) and applied stepwise regression. On the contrary, independent samples returned increased accuracy levels on ($R^2=0.83$) when applying an extended set of environmental parameters and one RS data set in a neural network (Akramkhanov and Vlek 2012). However, the number of samples available exceeded that of this study by a factor of five, which may have increased confidence of prediction. In general, absolute comparisons of the results achieved here remain difficult as long as methods, data sets, temporal and spatial scales of analyses in other studies differ.

The validation procedure underlined that multi-temporal data outperform mono-temporal data in modelling soil salinity. The variable importance analysis (except for 2009) suggests the consideration of RS data at the initial peak of the

irrigation period in July (Tischbein et al. 2013). In addition, the low model performance in 2011, when only few satellite data sets were available in the main irrigation phases, suggests (1) that the data of the early season (crop emergence) do only minor contribute and (2) that the selected environmental parameters alone could not predict soil salinity alone.

4.2 Limitations of the Approach

High inter-annual variation of RS data availability challenges rigorous comparisons among the annual models. For instance, it remains under discussion if the outstanding model performance in terms of RMSE and R^2 obtained for 2008 and 2011 can be attributed to water scarcity in the Amu Darya catchment (Conrad et al. 2016b) or not. One explanation could be low groundwater levels in those water scarce years, which in turn reduced capillary rise and hence soil salinity, and improved crop growth. However, salinity levels found for 2009 and 2010 exceeded that of 2008 and 2011, i.e. years of high water availability (Akramkhanov et al. 2014).

The variable importance assessments were based on RF according to Breiman (2001). But in these classical recursive partitioning approaches variable selection bias towards covariates with many possible splits may be observed, which in turn can seriously affect the interpretability of tree-structured regression models (Hothorn et al. 2006). The fact that

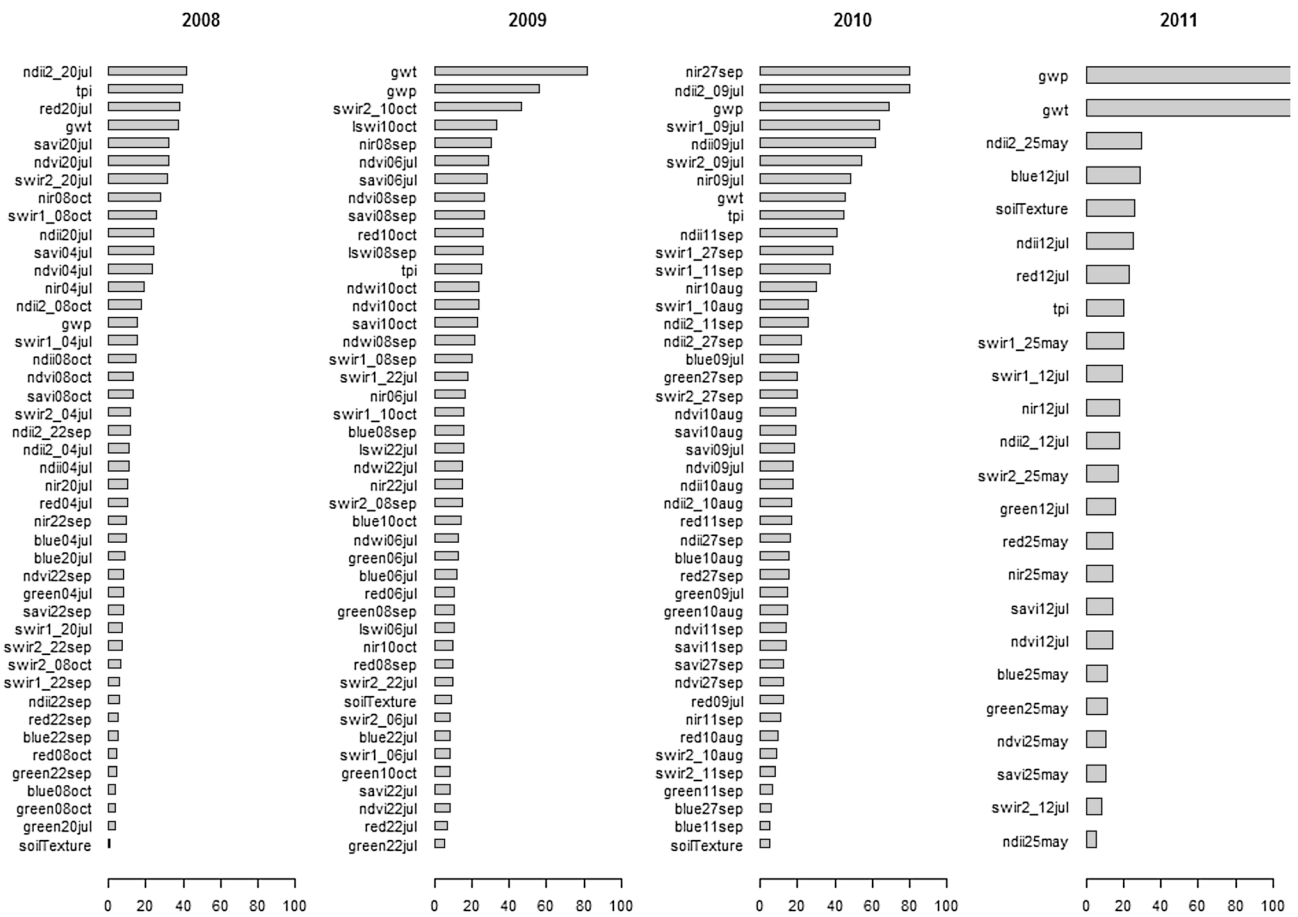
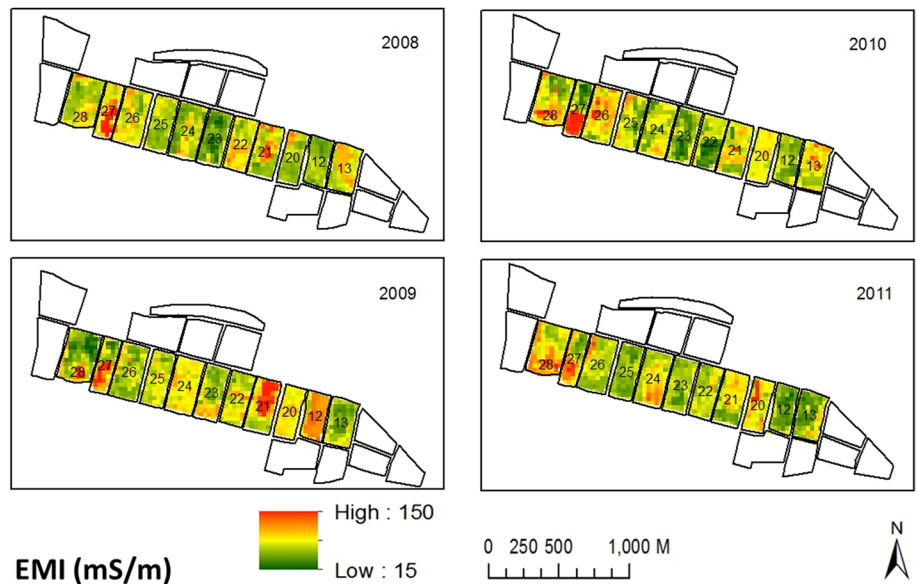


Fig. 7 Average variable importance (%IncMSE) received from the random forest applications for the multi-temporal data and the environmental parameters

Fig. 8 Spatial distribution of electromagnetic induction (EMI) at the end-of-season for the years 2008–2011. Results from the random forest applications for the multi-temporal data and the environmental parameters are depicted



the direction of the relation between predictor variables and soil salinity as results from multivariate ordinary last square regression (Akramkhanov et al. 2011) could not be measured

by the selected variable importance method may be another methodological limitation and call for further research, e.g. the comparison of different statistical approaches.

The comparatively small and thus environmentally homogenous study area very likely challenges the extrapolation of the results. Even though the study covered major crops of the ASB (L ow et al. 2015), variations of soils, groundwater water conditions (irrigation amounts and scheduling), and crop phenology limit the transferability. However, the results indicate that multi-temporal RS can compensate some variations and future research on a bigger area extent may require additional indicators including soil texture zones or distances to the irrigation and drainage infrastructure as previously shown by Akramkhanov and Vlek (2012) at the district level. The same step may also reduce the unexplained variance of the RF models in this study.

Rhoades et al. (1992) highlighted remarkable differences for the relative salt tolerance between crops to the level of salinity and salinity types. Also previous studies report complication of RS-based approaches due to the variations of crops in their salt tolerance (Allbed and Kumar 2013). These facts may be reason for the unexplained variance of the model in this study, which was applied to cotton and maize simultaneously. Interestingly, models applied to cotton fields of CRS only (not presented here) showed similar results and slightly underperformed the model ensemble applied to all fields. However, the model is very likely not applicable to soil under crops different to those included in this study.

4.3 Practical Implications

In Uzbekistan, official salinity measurements are conducted after summer season for managing the leaching of salts during winter rest (Ibrakhimov et al. 2011). In situ soil samples and laboratory assessments of electric conductivity (EC) serve for this purpose (Akramkhanov et al. 2008). The electromagnetic induction (EMI) approach, e.g. using the EM-38, can supplement these samplings because it is less time and cost consuming (Akramkhanov et al. 2008) and can be translated to EC (Akramkhanov et al. 2011). Moreover, together with spatial interpolation such as kriging it allows for assessments on larger scale

(Akramkhanov et al. 2011; Akramkhanov and Vlek 2012). However, the study at hand underlines the usefulness of RS for the prediction of EMI to account for the patchy structure of salinization patterns that typically occur in Uzbekistan (Shirokova et al. 2000), maybe even better than statistical interpolation, which in turn should be subject to future research.

Against this background, and for assessing the practicability of the multi-temporal RS approach, the EMI measurements and the model outputs at all sample sites were translated to EC using the existing transfer function (see Sect. 2.3) (Akramkhanov et al. 2014). Because decisions are taken based on salinity levels, both EC values based on model predictions and EMI measurements were classified according to the local standards (Table 4). Analysing the confusion matrix, i.e. the calculation of the overall accuracy according to Congalton and Green (2008), revealed that the three salinity classes applied in Uzbekistan could be met on ~80% of the EMI sample sites. In the water abundant year 2010 (Conrad et al. 2016b) confusion and overestimation occurred mainly among medium and low salinity classes and reduced the overall accuracy to 76%.

5 Conclusion

This research aimed at improved salinity assessment in irrigation systems without functioning drainage and with shallow groundwater levels at the end of cropping season through combinations of multi-temporal remote sensing (RS) and environmental parameters and using random forest. The methods were tested on a farm in Uzbekistan, where frequent in situ observations of EMI were available for 2008–2011. Multi-temporal RS information exceeded the performance of mono-temporal data. Increased R^2 and reduced RMSE clearly show that inclusion of environmental indicators improves the prediction of soil salinity. Multi-temporal remote sensing data sets especially from the main irrigation and growing phases may replace some,

Table 4 Confusion matrix between on model outputs and EMI transferred to EC values and classified into different soil salinity classes

Year (RF model)	2008				2009				2010				2011			
	L	M	H	PA (%)	L	M	H	PA (%)	L	M	H	PA (%)	L	M	H	PA (%)
L	27	29	1	47	5	20	1	19	4	30	1	11	21	38	1	35
M	2	147	22	86	1	69	22	75	0	34	19	64	0	173	9	95
H	0	12	139	92	0	7	157	96	0	2	131	98	0	19	119	86
UA (%)	93	78	86		83	72	87		100	52	87		100	75	92	
Overall Acc. (%)	83				82				76				82			

The confusion matrix and the error analysis are described in Congalton and Green (2008)

L low (0–4 dSm⁻¹), *M* medium (4–8 dSm⁻¹), *H* high (8–16 dSm⁻¹), *PA* producer’s accuracy, *UA* user’s accuracy

even though not all environmental factors in modelling soil salinity and vice versa.

Scientific comparison of the results with those reported from other areas is limited. The discussion suggests to having common concepts and standards in modelling of soil salinity. Besides exact documentation of in situ data, sampling design and the model especially the validation based on independent data are requested because the latter is the only requirement to assess the prediction quality and hence the suitability of an approach for extrapolation.

Uncertainties in the RS approach remain from the unexplained variances (R^2), which may be overcome by the inclusion of additional data (e.g. distance to the irrigation and drainage infrastructure), or through improved considerations of physical, vertical processes in the formulation of predictor variables, e.g. by modelling.

The study underpinned that the approach can support predictions of EMI at unvisited locations however; variable availability of optical RS data among the years limits its temporal transferability of the model and demands a year-to-year establishment of a new prediction model. In addition, the comparatively homogenous small study site calls for further experiments of the presented approach at larger scales and sampling especially in areas of high or low salinity.

Nevertheless, plausible prediction of EC levels indicates certain practical applicability of modelling end-of-season soil salinity through multi-temporal RS and environmental parameters. Together with in situ measurements of EC and EMI, these methods may contribute to formulate urgently required, site-specific strategies to cope with salinity in the entire ASB, and beyond.



Acknowledgements This research is a part of the joint project “Assessing Land Value Changes and Developing a Discussion-Support-Tool for Improved Land Use Planning in the Irrigated Lowlands of Central Asia” (LaVaCCA), funded by the Volkswagen Foundation (Az. 88506).

References

- Abbas A, Khan S (2007) Using remote sensing techniques for appraisal of irrigated soil salinity. In: Oxley L, Kulasiri D (eds) *Advances and applications for management and decision making land, water and environmental management: integrated systems for sustainability MODSIM07*, pp 2632–2638
- Abrol IP, Yadav JSP, Massoud FI (1988) Salt-affected soils and their management. *FAO Soils Bulletin* 39. Food and Agriculture Organization of the United Nations, Rome. <http://www.fao.org/docrep/x5871e/x5871e00.htm#Contents>. Accessed 22 Oct 2018
- AghaKouchak A, Farahmand A (2015) Remote sensing of drought: progress, challenges and opportunities. *Rev Geophys* 53:452–480. <https://doi.org/10.1002/2014rg000456>
- Akramkhanov A, Vlek PLG (2012) The assessment of spatial distribution of soil salinity risk using neural network. *Environ Monit Assess* 184(4):2475–2485. <https://doi.org/10.1007/s10661-011-2132-5>
- Akramkhanov A, Sommer R, Martius C, Hendrickx JMH, Vlek PLG (2008) Comparison and sensitivity of measurement techniques for spatial distribution of soil salinity. *Irrig Drain Syst* 22(1):115–126. <https://doi.org/10.1007/s10795-008-9043-9>
- Akramkhanov A, Martius C, Park SJ, Hendrickx JMH (2011) Environmental factors of spatial distribution of soil salinity on flat irrigated terrain. *Geoderma* 163(1–2):55–62. <https://doi.org/10.1016/j.geoderma.2011.04.001>
- Akramkhanov A, Kuziev R, Sommer R, Martius C, Forkutsa O, Mas-sucati L (2012) Soils and soil ecology in Khorezm. In: Martius C, Rudenko I, Lamers JPA, Vlek PLG (eds) *Cotton, water, salts and soums: economic and ecological restructuring in Khorezm, Uzbekistan*. Springer Netherlands, Dordrecht, pp 37–58. https://doi.org/10.1007/978-94-007-1963-7_3
- Akramkhanov A, Brus DJ, Walvoort DJJ (2014) Geostatistical monitoring of soil salinity in Uzbekistan by repeated EMI surveys. *Geoderma* 213:600–607
- Allbed A, Kumar L (2013) Soil salinity mapping and monitoring in arid and semi-arid regions using remote sensing technology: a review. *Adv Remote Sens* 2:373–385
- Asfaw E, Suryabagavan KV, Argaw M (2018) Soil salinity modeling and mapping using remote sensing and GIS : the case of Wonji Sugar Cane Irrigation Farm. Ethiopia. *J Saudi Soc Agric Sci* 17(3):250–258. <https://doi.org/10.1016/j.jssas.2016.05.003>
- Azabdaftari A, Sunar F (2016) Soil salinity mapping using multi-temporal landsat data. *Int Arch Photogramm Remote Sens Spat Inf Sci ISPRS Arch* 41:3–9. <https://doi.org/10.5194/isprsarchives-xli-b7-3-2016>
- Bastiaanssen WGM, Allen RG, Droogers P, D’Urso G, Steduto P (2007) Twenty-five years modeling irrigated and drained soils: state of the art. *Agric Water Manag* 92(3):111–125. <https://doi.org/10.1016/j.agwat.2007.05.013>
- Breiman L (2001) Random forests. *Mach Learn* 45(1):5–32
- Brower C, Goffeau A, Heibloem M (1985) *Irrigation water management: Training Manual No. 1—introduction to irrigation*. FAO—Food and Agriculture Organization of the United Nations (Rome), Rome
- Congalton RG, Green K (2008) *Assessing the accuracy of remotely sensed data: principles and practices*, vol 2. CRC Press, Boca Raton
- Conrad C, Schorcht G, Tischbein B, Davletov S, Sultonov M, Lamers JPA (2012) Agro-meteorological trends of recent climate development in Khorezm and implications for crop production. In: Martius C, Rudenko I, Lamers JPA, Vlek PLG (eds) *Cotton, water, salts and soums: economic and ecological restructuring in Khorezm, Uzbekistan*, vol 9789400719. https://doi.org/10.1007/978-94-007-1963-7_2
- Conrad C, Lamers JPA, Ibragimov N, Löw F, Martius C (2016a) Analysing irrigated crop rotation patterns in arid Uzbekistan by the means of remote sensing: a case study on post-Soviet agricultural land use. *J Arid Environ* 124:150–159. <https://doi.org/10.1016/j.jaridenv.2015.08.008>
- Conrad C, Schönbrodt-Stitt S, Löw F, Sorokin D, Paeth H (2016b) Cropping intensity in the aral sea basin and its dependency from the runoff formation 2000–2012. *Remote Sens* 8(8):630. <https://doi.org/10.3390/rs8080630>
- Dehaan RL, Taylor GR (2002) Field-derived spectra of salinized soils and vegetation as indicators of irrigation-induced soil salinization. *Remote Sens Environ* 80(3):406–417. [https://doi.org/10.1016/S0034-4257\(01\)00321-2](https://doi.org/10.1016/S0034-4257(01)00321-2)
- Eldeiry AA, Garcia LA (2008) Detecting soil salinity in alfalfa fields using spatial modeling and remote sensing. *Soil Sci Soc Am J* 72(1):201–211. <https://doi.org/10.2136/sssaj2007.0013>
- Farifteh J, Van der Meer F, Atzberger C, Carranza EJM (2007) Quantitative analysis of salt-affected soil reflectance spectra: a comparison of two adaptive methods (PLSR and ANN). *Remote Sens Environ* 110(1):59–78. <https://doi.org/10.1016/j.rse.2007.02.005>

- Farifteh J, Van der Meer F, van der Meijde M, Atzberger C (2008) Spectral characteristics of salt-affected soils: a laboratory experiment. *Geoderma* 145:196–206. <https://doi.org/10.1016/j.geoderma.2008.03.011>
- Gislason PO, Benediktsson JA, Sveinsson JR (2006) Random forests for land cover classification. *Pattern Recognit Lett* 27(4):294–300. <https://doi.org/10.1016/j.patrec.2005.08.011>
- Hendrickx JMH, Baerends B, Raza ZI, Sadig M, Akram Chaudhry M (1992) Soil salinity assessment by electromagnetic induction of irrigated land. *Soil Sci Soc Am J* 56(6):1933–1941. <https://doi.org/10.2136/sssaj1992.03615995005600060047x>
- Hillel D (2000) *Salinity management for sustainable irrigation. Integrating science, environment, and economics*. Washington, DC, USA
- Hothorn T, Hornik K, Zeileis A (2006) Unbiased recursive partitioning: a conditional inference framework. *J Comput Graph Stat* 15(July):651–674. <https://doi.org/10.1198/106186006X133933>
- Huang J, Prochazka MJ, Triantafyllis J (2016) Irrigation salinity hazard assessment and risk mapping in the lower Macintyre Valley, Australia. *Sci Total Environ* 551–552:460–473. <https://doi.org/10.1016/j.scitotenv.2016.01.200>
- Huete AR (1988) A Soil-Adjusted Vegetation Index (SAVI). *Remote Sens Environ* 25(3):295–309
- Ibrakhimov M, Khamzina A, Irina Forkutsa G, Paluasheva JPA, Lamers B, Tischbein PLG, Vlek PLG, Martius C (2007) Groundwater table and salinity: spatial and temporal distribution and influence on soil salinization in Khorezm Region (Uzbekistan, Aral Sea Basin). *Irrig Drain Syst* 21(3–4):219–236. <https://doi.org/10.1007/s10795-007-9033-3>
- Ibrakhimov M, Martius C, Lamers JPA, Tischbein B (2011) The dynamics of groundwater table and salinity over 17 years in Khorezm. *Agric Water Manag* 101(1):52–61. <https://doi.org/10.1016/j.agwat.2011.09.002>
- Ittersum MK, Cassman KG, Grassini P, Wolf J, Tittonell P, Hochman Z (2013) Field crops research yield gap analysis with local to global relevance—a review. *Field Crops Res* 143:4–17. <https://doi.org/10.1016/j.fcr.2012.09.009>
- Jabbarov H (1990) *The analysis of the indicators of ameliorative conditions in irrigated Areas of Khorezm Region*. Ph.D. Thesis, NPO SANIIRI, Tashkent Uzbekistan
- Keeley JE (2009) Fire intensity, fire severity and burn severity: a brief review and suggested usage. *Int J Wildland Fire* 18(1):116–126. <https://doi.org/10.1071/WF07049>
- Lobell DB, Ivan Ortiz-Monasterio J, Gurrola FC, Valenzuela L (2007) Identification of saline soils with multiyear remote sensing of crop yields. *Soil Sci Soc Am J* 71(3):777. <https://doi.org/10.2136/sssaj2006.0306>
- Löw F, Knöfel P, Conrad C (2015) Analysis of uncertainty in multi-temporal object-based classification. *ISPRS J Photogramm Remote Sens* 105:91–106. <https://doi.org/10.1016/j.isprsjprs.2015.03.004>
- Majka D, Jenness J, Beier P (2007) *CorridorDesigner: ArcGIS tools for designing and evaluating corridors*. <http://corridordesign.org>. Accessed 22 Oct 2018
- Masek JG, Vermote EF, Saleous N, Wolfe R, Hall FG, Huemmrich KF, Gao F, Kutler J, Lim TK (2013) LEDAPS calibration, reflectance, atmospheric correction preprocessing code, version 2. ORNL Distributed Active Archive Center. <https://doi.org/10.3334/ornldaac/1146>
- Metternicht GI, Zinck JA (2003) Remote sensing of soil salinity: potentials and constraints. *Remote Sens Environ* 85:1–20. [https://doi.org/10.1016/S0034-4257\(02\)00188-8](https://doi.org/10.1016/S0034-4257(02)00188-8)
- Qadir M, Noble AD, Qureshi AS, Gupta RK, Yuldashev T, Karimov A (2009) Salt induced land and water degradation in the aral sea basin: a challenge to sustainable agriculture in central Asia. *Nat Resour Forum* 33(2):134–149. <https://doi.org/10.1111/j.1477-8947.2009.01217.x>
- Rhoades JD, Kandiah A, Mashali AM (1992) *The use of saline waters for crop production*. FAO Irrigation and Drainage Paper, vol 48
- Rouse JW, Haas RH, Schell JA, Deering DW (1974) Monitoring vegetation systems in the great plains with ERTS. In: *Third earth resources technology satellite-1 symposium, vol I: technical presentations*. NASA SP-351, pp 309–317
- Shepard D (1968) A two-dimensional interpolation function for irregularly-spaced data. In: *Proceedings of the 1968 ACM national conference*, pp 517–524. <https://doi.org/10.1145/800186.810616>
- Shirokova Y, Forkutsa I, Sharafutdinova N (2000) Use of electrical conductivity instead of soluble salts for soil salinity monitoring in Central Asia. *Irrig Drain Syst* 14(3):199–205. <https://doi.org/10.1023/A:1026560204665>
- Stolbovoi V (2000) Soils of Russia: correlated with the revised legend of the FAO soil map of the world and world reference base for soil resources
- Tischbein B, Manschadi AM, Conrad C, Hornidge A-K, Bhaduri A, Ul Hassan M, Lamers JPA, Awan UK, Vlek PLG (2013) Adapting to water scarcity: constraints and opportunities for improving irrigation management in Khorezm, Uzbekistan. *Water Sci Technol Water Supply* 13(2):337. <https://doi.org/10.2166/ws.2013.028>
- Xiao XM, Boles S, Liu JY, Zhuang DF, Froelking S, Li CS, Salas W, Moore B (2005) Mapping paddy rice agriculture in southern China using multi-temporal MODIS images. *Remote Sens Environ* 95(4):480–492

Affiliations

Murodjon Sultanov¹ · Mirzakhayot Ibrakhimov¹ · Akmal Akramkhanov²  · Christian Bauer³ · Christopher Conrad^{3,4} 

✉ Christopher Conrad
christopher.conrad@uni-wuerzburg.de

¹ Khorezm Rural Advisory Support Service (KRASS), 14, Khamid Olimjan Street, 220100 Urgench, Khorezm, Uzbekistan

² International Center for Agricultural Research in the Dry Areas (ICARDA), P.O. Box 4375, 100000 Tashkent, Uzbekistan

³ Remote Sensing Department, University of Würzburg, Institute of Geography and Geology, Oswald-Külpe-Weg 86, 97074 Würzburg, Germany

⁴ University of Halle-Wittenberg, Institute of Geosciences and Geography, Von-Seckendorff-Platz 4, 06120 Halle, Germany